J. Astrophys. Astr. (2000) **21**, 265-268

Tessellation of SoHO Magnetograms

R. Srikant* & Jagdev Singh, *Indian Institute of Astrophysics, Bangalore 560034, India*
**e-mail: srik@iiap.ernet.in*

Abstract. A gradient based algorithm which divides arbitrary images into non-overlapping surface filling tiles of opposite polarity is used to study the flux and size distributions of large scale magnetic flux concentrations in solar and heliospheric observatory (SoHO) magnetograms. The mean absolute flux and size of the concentrations at the considered scale is found to be about 1.7×10^{18} Mx and 5.2 Mm for both polarities. The form of the flux distribution is characterized by a skewness of $\alpha_3 = 4.9$ and a kurtosis of $\alpha_4 = 42.8$. The fall in the distribution in the range 6.5×10^{17} Mx to 5×10^{18} Mx is described by an exponential fit, in agreement with a model for the sustenance of quiet region flux.

Key words. Sun: granulation—magnetogram.

1. Introduction

The structure of magnetic flux on the solar surface is the result of the interaction of magnetic fields with the convective flows. Magnetic flux is not uniformly distributed, but, even at the scale of a few arcsecs, parcelled into flux concentrations with flux of the order of 10^{18} Mx. As a result of buffetting by granules, shear in the flow in which the concentrations are embedded, these concentrations constantly evolve by colliding, merging, cancelling and fragmenting (Martin 1990). The histogram of flux in concentrations is an effect of these processes, and can hence shed light on them. Here we describe a method to study flux concentrations statistically.

2. Data analysis

The data consists of full disk magnetograms from the Solar and Heliospheric Observatory (SoHO)/Michelson Doppler Imager (MDI) extending over 10.5 hr. A magnetogram is subjected to a procedure, whereby it is mapped into a pattern of surface filling non-overlapping tiles. In the version of the method followed by Hagenaar *et al.* (1997) and Srikanth *et al.* (2000), the local minima in the magnetogram are identified. Then, those pixels converging towards a given minimum according to the steepest descent criterion are collected into a single tile labelled by that minimum. This results in the entire image being tessellated. Fig. 1 is a result of the tessellation of a quiescent window of size 160" × 160".

Adapting the tessellation procedure to magnetograms requires a non-trivial extension in order to take into account the bipolarity of magnetic fields. The new method

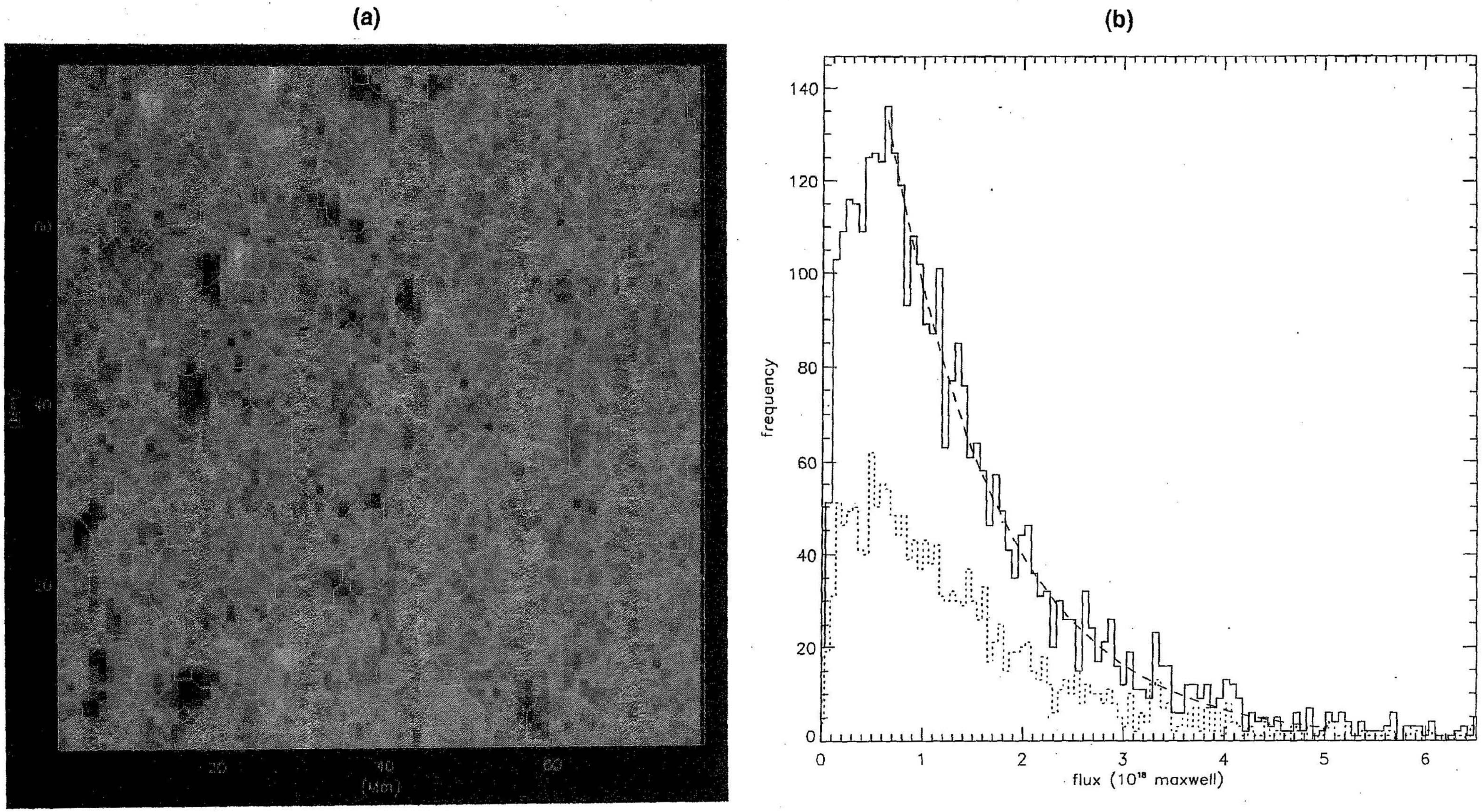

Figure 1. (**a**) Tessellation of a magnetogram window, with tiles enclosing positive and negative flux regions; when two same-signed extrema occur close to each other, the tile boundary apparently cuts through concentrations; (**b**) Histogram of the flux concentrations; the large histogram represents the combined flux values for both polarities, with an exponential fit indicated in the range 0.64×10^{18} to 5×10^{18} Mx. The smaller dotted histogram represents positive polarity flux concentrations.

consists in doubly tessellating the image: first, to determine the local minima and their associated tessellation according to steepest descent; and second, to determine the local maxima, and analogously their associated tessellation via 'steepest ascent', wherein the locus of a point is along the direction of the highest positive gradient. The part of the image covered by negative valued pixels in the first tessellation describes the discontinuous system of negative flux concentrations. Its exact area and flux complement is given by the part of the image covered by the positive valued pixels in the second tessellation. It might appear, at first, that the tessellation could be used to tile supergranules, given that supergranular outflows concentrate relatively large (mixed polarity) fields at their boundaries. However, this is thwarted by the discrete character of the flux. The tiles that constitute the tessellation are interpreted as flux concentrations. Their boundaries are neutral lines where the field changes sign.

Two advantages of the present method: (1) In the related work of Schrijver *et al.* (1997), the total flux of the concentrations is determined assuming the net flux as being three times the core flux. No such (possibly model dependent) assumption is made here. The total flux is obtained by integrating the absolute field over the tile; (2) We have a direct handle of the size of the concentrations, which can be used for geometric modelling of the latter.

For the present study, a total of seven such windows spanning about 10.5 hours of data were used. A total of 3559 tiles were obtained by the double tessellating procedure, with 1775 and 1784 tiles carrying negative and positive flux, respectively. Both temporal averaging and spatial smoothing of magnetograms increase the mean size of the observed tiles, by suppressing small-scale and short-term fluctuations (Srikanth *et al.* 2000).

3. Results

Fig. 1(b) is the histogram of the tiles obtained from the double tessellation of SoHO magnetograms. The bold outline represents the combined graph for both polarities. The other represents the positive polarity taken separately. The distribution peaks around 6.4×10^{17} Mx, in agreement with the value obtained by Schrijver *et al.* (1997) for core fluxes, and not incompatible with that of Wang *et al.* (1995). The flux distribution function of the tiles is characterized by its skewness (α_3) (asymmetry) and kurtosis (α_4) (peakedness) given by:

$$\alpha_m = \frac{1}{n\sigma^m}\left(\sum_i (x_i - \bar{x})^m\right) \tag{1}$$

where σ is standard deviation. The mean flux, mean size, skewness and kurtosis for the positive, negative and combined flux concentrations are given in Table 1.

The mean absolute flux value of Γ.7 $\times$ 10^{18}Mx, confirms earlier estimates. The larger mean compared to the mode of the distribution is reflected in the positive skewness of the flux distribution. As expected, the characteristics of the distribution are similar for both polarities. The mean size of the concentration emerges at about 5 Mm, suggesting that the tiles may be identified with large network elements. This somewhat large value, and its closeness to mesogranular size (Ploner *et al.* 2000), are points that merit further investigation. This size implies a mean flux for the quiet region of about 2.2 gauss (LaBonte & Howard 1980).

Table 1. Mean tile flux, size, and skewness and kurtosis of flux distributions of positive, negetive and combined flux concentrations from SoHO magnetograms.

Type	Mean abs. flux	Mean size	Skewness	Kurtosis
Positive	1.7×10^{18} Mx	5.3 Mm	4.8	42.2
Negative	1.6×10^{18} Mx	5.1 Mm	5.0	43.3
Combined	1.7×10^{18} Mx	5.2 Mm	4.9	42.8

4. Discussion and conclusions

We find that an exponential fit well describes the fall in the distribution function in Fig. 1(b) in the range between 6.4×10^{17} and 5×10^{18} The exponential character extends below the 10^{18} Mx point noted by Schrijver *et al.* (1997). According to their empirical model for the dynamics and sustenance of flux in quiet regions, this supports the scenario that flux concentrations are subject to fragmentation and that re-emergent flux is not entirely derived from previously cancelled flux. New flux from ephemeral regions accounts for the remaining flux required to sustain the quiet network. For values of flux smaller than 10^{17}, the noise in the data (about 2.5×10^{16} Mx per pixel) renders small magnetic concentrations unobservable. The turn-down from the exponential fit is, therefore, perhaps an artifact of the data, rather than intrinsic to the magnetic flux.

The present method can help us look for possible clustering properties among like-polarity concentrations. In future work, we will relate the large value of the kurtosis of the flux distribution to the flux-size relation, and hence, derive a geometrc model of the concentrations.

Acknowledgements

We thank Dr. P. H. Scherrer and the SoHO consortium for providing us with the MDI/ SOI magnetogram data.

References

Hagenaar, H. J., Schrijver, C. J., Title, A. M. 1997, *Astrophys. J.,* **481,** 988.
LaBonte, B. J., Howard, R. 1980, *Sol. Phys.,* **80,** 15.
Martin, S. F 1990, in *Solar Photosphere: Structure, Convection, and Magnetic Fields, IAU Symp. 138,* (ed) Stenflo, J. O. (Dordrecht: Kluwer) 129.
Ploner, S. R. O., Solanki, S. K., Gadun, A. S. 2000, *Astron. Astrophys.,* **356,** 1050.
Schrijver, C. J., Title, A. M., Ballegooijen, A., Hagenaar, H. J., Shine, R. 1997, *Astrophys. J.,* **481,** 424.
Srikanth, R., Singh, J., Raju, K. P. 2000, *Astrophys. J.,* **534,** 1008.
Wang, J., Wang, H., Tang, F, Lee, J. W., Zirin, H. 1995, *Sol. Phys.,* **160,** 277.